

# GIBBS-WEIGHTED K-MEANS SEGMENTATION APPROACH WITH INTENSITY INHOMOGENEITY CORRECTION

Chia-Yen Lee<sup>1</sup>, Chiun-Sheng Huang<sup>2</sup>, Yeun-Chung Chang<sup>3</sup>, Yi-Hong Chou<sup>4</sup> and Chung-Ming Chen<sup>1</sup>

<sup>1</sup>*Institute of Biomedical Engineering, National Taiwan University, Taipei, Taiwan*

<sup>2</sup>*Department of Surgery, National Taiwan University Hospital, Taipei, Taiwan*

<sup>3</sup>*Department of Medical Imaging, National Taiwan University Hospital, Taipei, Taiwan*

<sup>4</sup>*Department of Radiology, Taipei Veterans General Hospital, Taipei, Taiwan*

**Keywords:** Breast Sonogram, Intensity Inhomogeneity Correction, Segmentation, Fuzzy Cell Competition, Clustering.

**Abstract:** Intensity inhomogeneity caused by an ultrasonic attenuation beam within the body results in an artifact effect. It frequently degrades the boundary and texture information of a lesion in a breast sonogram. A new Gibbs-weighted K-means segmentation approach with intensity inhomogeneity correction is proposed to cluster the prominent components provided by fuzzy cell competition algorithm for segmenting lesion boundaries automatically with reducing the influence of the intensity inhomogeneity. The information of fuzzy C-means, normalized cut, and cell-based fuzzy cell competition algorithm are combined as the feature vector for cell-based clustering. 49 breast sonograms with intensity inhomogeneity, each from a different subject, are randomly selected for performance analysis. The mean distance between the lesion boundaries attained by the proposed algorithm and the corresponding manually delineated boundaries defined by two radiologists is  $1.571 \pm 0.513$  pixels. (Assessing Chan and Vese level set method for intensity inhomogeneity-correction segmentation in the same way, the mean distance error is  $3.299 \pm 1.203$  pixels, for the 49 images.) The results show that Gibbs-weighted K-means segmentation approach with intensity inhomogeneity correction could not only correct the intensity inhomogeneity effect but also improve the segmentation results.

## 1 INTRODUCTION

Boundary segmentation is an essential step for the quantitative analysis of sonographic breast lesions. The shape and contour of the lesion are important indicators for the malignancy of breast lesions. Varieties of approaches have been proposed for segmentation of sonographic breast lesions. Despite the satisfactory performances that have been repeatedly reported, each class of algorithms suffer certain types of fundamental deficiency and boundary delineation of sonographic breast lesions remains as a hard task in general. For example, for a breast lesion with a complex texture pattern in the vicinity of the lesion boundary, the deformation of the deformable models (Chen, 2003) and level-set methods (Chan, 2001) is easily blocked by the textural structures or leaks out from the weak edges (Chen, 2005).

A cell-based approach, Gibbs-weighted K-means segmentation approach with intensity inhomogeneity

correction, is proposed instead of the conventional pixel-based approaches. Based on cell-based concept, one important part of proposed approach, fuzzy cell competition algorithm, is applied to identify all prominent components in an ROI simultaneously. A *prominent component* is the substructure of a tissue or a part of breast lesion with a visually perceivable boundary. In general, each breast lesion is composed of a very limited number of prominent components, with which the lesion boundary can be easily derived by a boundary delineation approach, e.g., cell-based clustering.

In that way, the Gibbs-weighted K-means segmentation approach with intensity inhomogeneity correction combines the information of each prominent component computed by fuzzy c-means, normalized cut, and cell-based fuzzy cell competition algorithm as the feature vector for cell-based clustering. However, intensity inhomogeneity, which may be composed of acoustic shadow and enhancement, is a common artifact in a breast

sonogram. Intensity inhomogeneity may also degrade the boundary and texture information. The typical example is the shadowing artifact may result in weak edges or missing edges, aggravating the difficulty of extracting the lesion boundaries for further lesion characterization.

In a breast sonogram, an ultrasonic beam may travel through several different tissues, such as fat, muscle, mammary gland, lesion, and so on. Moreover, the composition of tissue types along the traversing path varies with ultrasonic beams. It suggests that the attenuation effect is basically spatially-variant, which is not only a function of traveling distance but also a function of ultrasonic beam. To reduce the influence of intensity inhomogeneity in breast sonograms, polynomial surface model (Lee, 2010) is applied to take into account the spatially-variant nature of the attenuation and minimize the probability of being trapped in a local minimum.

## 2 MATERIALS AND METHODS

The ROI is assumed to be composed of the foreground and background regions. Each region is assumed to be a homogeneous area with a mean intensity,  $\mu_\Psi$ ,  $\Psi \in \{F, B\}$ , where  $F$  and  $B$  denote the foreground and background regions, respectively. Let  $g_i$  denote the observed gray level of the  $i$ th pixel in the ROI. Then,  $g_i$  may be expressed as

$$g_i = \mu_\Psi + P_i + n_i \quad (1)$$

where  $\Psi \in \{F, B\}$  depending on the location of the  $i$ th pixel. The last two terms model the intensity inhomogeneity and the noise. The noise is assumed to be normally-distributed with zero mean. The intensity inhomogeneity in an ROI is modeled as a spatially-variant normal distribution with a constant variance and spatially-variant means, which forms a polynomial surface of order  $n$  denoted by  $P_i$  in Eq. (1). The last term  $n_i$  is the composition of the noise and the variation on the polynomial surface of the intensity inhomogeneity, which is also normally-distributed.

The proposed segmentation with intensity inhomogeneity correction scheme is formulated as an EM algorithm composed of two major parts, namely, Gibbs-weighted K-means segmentation algorithm for the E-step as well as inhomogeneity estimation and correction for the M-step. In the E-step, the Gibbs-weighted K-means segmentation

algorithm divides the ROI into reasonable foreground and background regions by the new Gibbs-weighted K-means segmentation algorithm taking the outputs of the fuzzy c-means, fuzzy cell-competition algorithm and normalized cut algorithm as the feature vectors. In the M-step, the  $n$ th order polynomial surface of the inhomogeneity field is estimated by using the least squared fitting. The iteration process terminates when the difference of the estimated fields derived in two consecutive iterations is stabilized.

### 2.1 E Step

Based on the intensity inhomogeneity derived in the previous M-step, the E-step aims to provide a segmentation estimation of the foreground and background regions close to the true partition as possible for the M-step by the Gibbs-weighted K-means segmentation algorithm. The proposed algorithm comprises three components: fuzzy cell competition (FCC), normalized cut (NC), fuzzy c means (FCM).

#### 2.1.1 Fuzzy Cell Competition

The goal of the FCC algorithm is to derive a minimum number of prominent components constituting the breast lesion in a breast sonogram. The FCC algorithm (Lee, 2010) is a cell-based segmentation algorithm designed to find all prominent components in an ROI, the boundaries of which coincide with the visually perceived boundaries.

The cost function of the FCC algorithm characterizes the overall regional homogeneity of all regions and the total boundary strength of all boundary segments, which are defined by the first and second terms, respectively, in Eq. (2) for the  $i$ th iteration with  $H = \max_{\forall b_j \in \Phi^i} \{-\log p_j\}$ :

$$E^i = \mathfrak{R}^i + \lambda_c \mathfrak{N}^i = \frac{1}{n\sigma^2} \sum_{\forall r_j^i \in \Theta^i} \rho^2(r_j^i) + \lambda_c \sum_{\forall b_k \in \Theta^i} \frac{(H + \log p_k)}{\sum_{\forall b_j \in \Theta^i} (H + \log p_j)} \quad (2)$$

and

$$\rho^2(r_j^i) = \left\{ \sum_h u_{hj}^i \left[ \sum_k (f_k(c_{hj}^i) - \mu(c_{hj}^i))^2 + (\mu(c_{hj}^i) - \mu(r_j^i))^2 \right] \right\} \quad (3)$$

subject to

$$\sum_{\forall r_j^i \in \Theta^i} u_{hj}^i = 1 \quad (4)$$

where

- $\Theta^i$  : the set of regions in the  $i$ th iteration;
- $n_j^i$  : the number of pixels enclosed by  $r_j^i$ ;
- $c_{hj}^i$  : the  $h^{\text{th}}$  cell of  $r_j^i$  in the  $i$ th iteration;
- $f_k(c_{hj}^i)$  : the gray level of the  $k^{\text{th}}$  pixel enclosed by  $c_{hj}^i$ ;
- $\mu(c_{hj}^i)$  : the mean gray levels of the pixels enclosed by  $c_{hj}^i$  and  $r_j^i$ , respectively;
- $n$  : the number of pixels within the ROI;
- $\sigma^2$  : the variance of the gray levels of the pixels within the ROI;
- $u_{hj}$  : the membership of cell  $j$  to region  $r_j^i$ ;
- $\Phi^0$  : the set of boundary segments on the boundaries identified by the second pass of watershed transformation;
- $b_j$  : the  $j^{\text{th}}$  boundary segment.

A boundary segment is a small portion of a regional boundary uniquely shared by two elementary cells residing within two different regions. The boundary strength of a boundary segment, denoted by  $p_j$ , is a measure of the statistical significance of difference between these two elemental cells. It is defined as the minimum of the p-values of three two-tailed Kolmogorov-Smirnov (KS) tests respectively comparing the gray level distributions of pixels in two elementary cells and those on the boundary segment. The probability of  $b_j$  being an edge is defined as  $(1 - p_j)$ . Moreover, the overall boundary strength of the regional contour  $C_\Gamma$  defined by a fuzzy class labeling  $\Gamma$  is defined as the joint probability of all boundary segments on  $C_\Gamma$  being edges, i.e.,  $\mathfrak{F}_\Gamma = \prod_{\forall b_j \in C_\Gamma} (1 - p_j)$ . The membership

function in each iteration may be derived as:

$$u_{hj} = \frac{\left[ \sum_k (f_k(c_{hj}^i) - \mu(c_{hj}^i))^2 + (\mu(c_{hj}^i) - \mu(r_j^i))^2 \right]^{\frac{-1}{(q-1)}}}{\sum_{\forall r_j^i \in \Theta^i} \left[ \sum_k (f_k(c_{hj}^i) - \mu(c_{hj}^i))^2 + (\mu(c_{hj}^i) - \mu(r_j^i))^2 \right]^{\frac{-1}{(q-1)}}} \quad (5)$$

### 2.1.2 Gibbs-weighted K-means Segmentation Algorithm

K-means aims to divide a dataset into several groups. It needs feature vectors as inputs and a cost function to define the quality of the partition result.

The Gibbs model is generally used to site labeling problem to build the spatial dependency of each neighboring site, i.e., pixel, edges, elements, and region (Mohamed, 2004) via the set of clique potentials. A Gibbs-weighted K-means is proposed to provide a more general and flexible method to make to 2D sonogram segmentation results better. The basic idea is minimizing a cost function shown as Eq. (6) which the sum of squares of the distances of each cell to the two cluster center, i.e., background and foreground. For the pre-defined cluster number  $K$ , the cost function is defined by

$$S_G = \sum_{k=1}^K \sum_{C_h \in C_k} G_w \left\| \mu(C_h^i) - \mu(C_k^i) \right\|^2 \quad (6)$$

where the Gibbs-weighted is as following

$$G_w = z^{-1} \exp(-U) \quad (7)$$

and the energy function is a sum of clique potentials  $V_{C_{hk}}$  over the set of all adjacent pairs of cells  $\Xi$ .

$$U = \beta \sum_{C_{hk} \in \Xi} V_{C_{hk}}(l_h) \quad (8)$$

The clique potential is with respect to its neighboring cell to be defined as:

$$V_{C_{hk}}(l_h) = 1 - \delta_{hk} \quad (9)$$

where

$$\delta_{hk} = \begin{cases} 0, & \text{if } l_h \neq l_k \\ 1, & \text{if } l_h = l_k \end{cases} \quad (10)$$

There are six parameters as the feature vector to be inputs. The first two parameters are the mean gray-level of each cell which obtained by fuzzy cell competition, which are cell-based features. The third and fourth parameters are the mean of membership function of each cell. The membership functions of each pixel is derived by fuzzy c means originally, and then transfer to cell-based features, i.e., the membership functions of each cell, via the cell information obtained by the fuzzy cell competition algorithm. The fifth and sixth parameters are the mean of the second smallest eigenvalue of each cell which derived by normalized cut algorithm via combing the cell information.

## 2.2 M Step

The aim of this step is to fit the intensity inhomogeneity field to a polynomial surface in a bipartite ROI based on the model given in Eq. (1). It is assumed that the mean of intensity inhomogeneity

$P_i$  of pixel  $i$ ,  $\forall i$ , may be modeled as a polynomial surface. To estimate the polynomial surface, a least squared fitting is employed to minimize the cost function:

$$\varepsilon^2 = \frac{1}{N} \sum_{\forall i} (g_i - \mu_{\psi} - P_i)^2 \quad (11)$$

where  $\mu_R = \mu_F$  if pixel  $i$  is in the foreground region and  $\mu_R = \mu_B$  if pixel  $i$  is in the background region. Moreover,  $P_i = f(x_i, y_i)$ , where  $f(x, y)$  is a polynomial function of order  $n$ . In this study,  $n$  is set to 6.

### 3 RESULTS AND CONCLUSIONS

Forty-nine breast sonograms with intensity inhomogeneity acquired from 1996 – 2004, each from a different subject, were randomly selected from the ultrasound image database in a teaching hospital in Taiwan. The assessment is performed based on the mean manually-delineated boundary of each lesion in a breast sonogram. Each lesion was demarcated by two graduate students and confirmed by two experienced radiologists with 10- and 28-year experience, respectively.

The mean distance between the lesion boundaries attained by the proposed algorithm and the corresponding manually delineated boundaries defined by two radiologists is  $1.571 \pm 0.513$  pixels. (Assessing Chan and Vese level set method for intensity inhomogeneity-correction segmentation in the same way, the mean distance error is  $3.299 \pm 1.203$  pixels, for the 49 images).

Figure 1 results of the proposed segmentation approach and Chan and Vese level set method applied on the intensity inhomogeneity image. Fig. 1 (a) shows the mean manually-delineated boundary of the sonographic breast lesion given in Fig. 1 (c), i.e., the original image.

Fig. 1(b) gives the intensity inhomogeneity field and Fig. 1(f) shows the inhomogeneity-corrected breast sonogram. The weak edge at the upper-right portion of the lesion boundary becomes manifested in the inhomogeneity-corrected breast sonogram. The boundary derived by the Chan and Vese level set method of the intensity inhomogeneity image and intensity inhomogeneity-corrected image are shown as Fig. 1 (e) and Fig. 1 (h), respectively. The Chan and Vese level set method fails to capture the upper-right portion of the lesion boundary which is a weak edge caused by the intensity inhomogeneity. Fig. 1 (d) and Fig. 1 (g) show the cells (i.e., the prominent

components) derived by the FCC algorithm in the intensity inhomogeneity image and intensity inhomogeneity-corrected image, respectively. The cell structures play the role of offering the feature vectors to Gibbs-weighted K-means segmentation algorithm, and the clustering result is shown as Fig. 1 (i). The boundary derived by Gibbs-weighted K-means segmentation algorithm is shown as Fig. 1 (j).

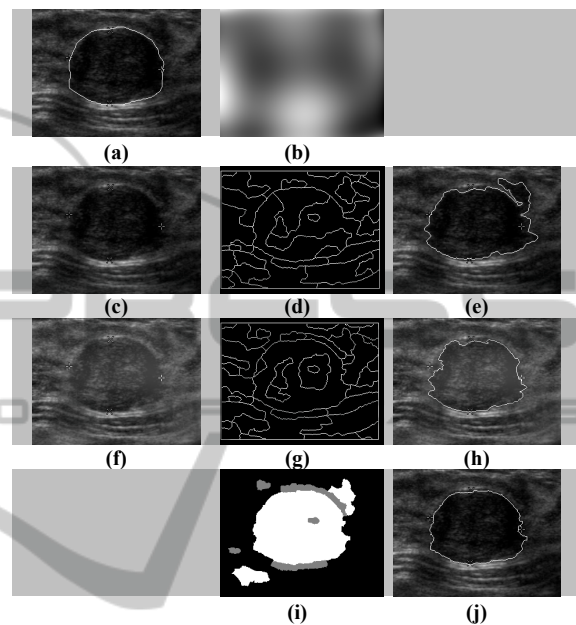


Figure 1: The proposed algorithm segmentation results compare with Chan and Vese level set method.

### REFERENCES

- Chan, T. F. and Vese, L. A., 2001. Active contours without edges. *IEEE Trans Image Processing* 10(2).
- Chen, C. M., Chou, Y. H. and Chen, C. S. K., 2005. Cell-competition algorithm: a new segmentation algorithm for multiple objects with irregular boundaries in ultrasound images. *Ultrasound in Medicine and Biology* 31(12).
- Chen, D. R., Chang, R. F., Wu, W. J., Moon, M. K. and Wu, W. L., 2003. 3-D breast ultrasound segmentation using active contour model. *Ultrasound in Medicine and Biology* 29(7).
- Lee, C. Y., Chou, Y. H., Huang, C. S., Chang, Y. C., Tiu, C. M., Chen, C. M., 2010. Intensity inhomogeneity correction for the breast sonogram: Constrained fuzzy cell-based bipartitioning and polynomial surface modeling. *Medical Physics* 37(11).
- Mohamed, R. M., El-Baz, A., and Farag A. A., 2004. Image Modeling Using Gibbs-Markov Random Field and Support Vector Machines Algorithm. *International Journal of Information Technology* 1(14).